



HAL
open science

Transport through a band insulator with Rashba spin-orbit coupling: metal-insulator transition and spin-filtering effects

Thibaut Jonckheere, George Japaridze, Thierry Martin, Roland Hayn

► **To cite this version:**

Thibaut Jonckheere, George Japaridze, Thierry Martin, Roland Hayn. Transport through a band insulator with Rashba spin-orbit coupling: metal-insulator transition and spin-filtering effects. *Physical Review B: Condensed Matter and Materials Physics (1998-2015)*, 2010, 81, pp.165443. 10.1103/PhysRevB.81.165443 . hal-00381501

HAL Id: hal-00381501

<https://hal.science/hal-00381501>

Submitted on 5 May 2009

HAL is a multi-disciplinary open access archive for the deposit and dissemination of scientific research documents, whether they are published or not. The documents may come from teaching and research institutions in France or abroad, or from public or private research centers.

L'archive ouverte pluridisciplinaire **HAL**, est destinée au dépôt et à la diffusion de documents scientifiques de niveau recherche, publiés ou non, émanant des établissements d'enseignement et de recherche français ou étrangers, des laboratoires publics ou privés.

**Transport through a band insulator with Rashba spin-orbit
coupling:
metal-insulator transition and spin-filtering effects**

T. Jonckheere,¹ G.I. Japaridze,² T. Martin,^{1,3} and R. Hayn⁴

¹*Centre de Physique Théorique, UMR 6207, case 907,
Campus de Luminy, 13288 Marseille Cedex 9, France*

²*Andronikashvili Institute of Physics,
Tamarashvili str. 6, 0177 Tbilisi, Georgia*

³*Université de la Méditerranée, Campus de Luminy, 13288 Marseille Cedex 9, France*

⁴*Institut Matériaux Microélectronique Nanosciences de Provence,
Faculté St. Jérôme, Case 142, F-13397 Marseille Cedex 20, France*

(Dated: May 5, 2009)

Abstract

We calculate the current-voltage characteristic of a one-dimensional band insulator with magnetic field and Rashba spin-orbit coupling which is connected to nonmagnetic leads. Without spin-orbit coupling we find a complete spin-filtering effect, meaning that the electric transport occurs in one spin channel only. For a large magnetic field which closes the band gap, we show that spin-orbit coupling leads to a transition from metallic to insulating behavior. The oscillations of the different spin-components of the current with the length of the transport channel are studied as well.

PACS numbers: 72.25.-b, 71.70.Ej

I. INTRODUCTION

There is a great interest today to study the phenomena of quantum transport in low dimensional systems, both from a technological and a fundamental point of view. Especially important are questions of spin polarized transport, also known as spintronics.¹ A famous example is the proposition of the Datta-Das transistor² which uses the rotation of the electron spin due to spin-orbit (SO) coupling. There are two sources of spin-orbit coupling in quasi one-dimensional systems (1D), an intrinsic one due to the lack of inversion symmetry in certain crystal structures (Dresselhaus term)³ and an external one triggered by an applied voltage to surface gates (the Rashba SO coupling).⁴

Several works studied the SO coupling and electronic transport in quasi 1D metallic systems.^{5,6,7,8,9,10,11,12,13,14,15,16} In contrast, the influence of SO coupling and magnetic field on the transport in 1D band insulators is unexplored, and it can be expected to be fundamentally different. In the letter band insulators, we will report on two interesting effects: the complete spin filtering effect and the SO induced metal-insulator transition. An incomplete spin filtering effect is possible in 1D metallic systems with a potential step or additional impurities,^{7,14,16} but the complete spin filtering as well as the spin-orbit induced metal-insulator transition which will be reported below are specific to 1D band insulators and cannot be observed (in principle) in 1D metals.

A prototype model for a one-dimensional (1D) band insulator is a half-filled ionic chain with alternating on-site energies (energy difference Δ). Such an ionic chain will be used in our study, however the obtained results are expected to be generic to any kind of 1D band insulators, including charge transfer insulators and realized in diatomic polymers,¹⁷ as well as the 1D Peierls insulators, such as polyacetylene.¹⁸ In a wider sense, one-dimensional band insulators may also be realized in carbon-nanotubes. These nanotubes have the advantage that the value of the gap may be tuned in a very wide range from 600 meV (for (12,0) nanotubes) up to 8 meV (for (13,0) nanotubes) or even smaller values.¹⁹

Before presenting detailed calculations, let us start with some qualitative arguments. We first discuss transport in 1D band insulators in a magnetic field B and in absence of SO interaction. Although the magnetic field induced metal-insulator and insulator-metal transitions have been the subject of studies for decades,²⁰ in the context of transport in mesoscopic systems these effects have not been investigated in detail. As we show in this

paper, in the limit of ultra-low temperatures ($T \ll \Delta$) and strong magnetic field ($B \geq \Delta$) the field induced insulator-metal transitions lead to the almost complete spin filtering effect, since in this case only one spin channel is open for transport at the Fermi level.

However, the metallic phase reached at $B \geq \Delta$ shows unconventional and substantially different properties compared to a normal metal. As we will show, contrary to the usual 1D metallic phase, the Rashba spin-orbit coupling opens up a gap again, leading to a spin-orbit induced metal-insulator transition. It is important to note that both effects, i.e. the complete spin filtering effect and the metal-insulator transition induced by the Rashba spin-orbit coupling are very specific to 1D band insulators, and may not be observed in 1D metals.

Rather than analyzing the effect of these transitions by computing the bulk transport properties of the chain, such as the conductivity, we choose to compute the current of a finite chain of such a material, whose extremities are connected to metallic electrodes. A bias is imposed between the electrodes in order to induce current flow. On the one hand it allows to probe the spin filtering effects in a setup which is close to experimental situations, on the other hand it also allows to investigate potential fluctuations of the current as a function of the chain length in the presence of SO coupling. In particular, we will show that a complex behavior, with several periods and a complicated energy dependence is obtained in the presence of a band gap Δ and a magnetic field; this is totally different from the simple harmonic oscillations, with a period inversely proportional to the SO coupling strength, obtained in the metallic case.

The paper is organized as follows. In Sec. II, we introduce the model and in Sec. III we discuss the spectrum of the infinite chain. In Sec. IV, we discuss the method which is used to obtain the transport properties as well as physical results. We conclude in Sec. V.

II. THE MODEL

We note first that the spin-orbit coupling can be generated by a voltage V_G applied to external gates perpendicular to the current. This is known as Rashba spin-orbit coupling,⁴ and defines the device studied in the present paper (Fig. 1). We consider a finite chain (oriented in the \hat{x} direction) connected to metallic leads. Lateral metallic gates are placed so that to create an electric field which is perpendicular to both the chain and the magnetic

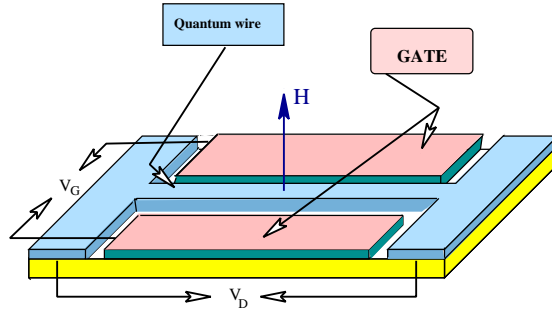


FIG. 1: (Color online) Schematic figure of the transport process studied in the paper. The SO coupling parameter α_R is proportional to V_G .

field (\hat{z}) direction. With these conventions the following Hamiltonian describes the molecular chain:

$$\begin{aligned}
 H = & -t \sum_{n,\sigma} (c_{n,\sigma}^\dagger c_{n+1,\sigma} + h.c.) + \frac{\Delta}{2} \sum_{n,\sigma} (-1)^n c_{n,\sigma}^\dagger c_{n,\sigma} \\
 & - \frac{g\mu_B H}{2} \sum_{n,\sigma} \sigma c_{n,\sigma}^\dagger c_{n,\sigma} \\
 & + \alpha_R \sum_n (c_{n,\uparrow}^\dagger c_{n+1,\downarrow} - c_{n,\downarrow}^\dagger c_{n+1,\uparrow} + h.c.) . \quad (1)
 \end{aligned}$$

Here the first contribution describes the kinetic energy in the tight binding model, the second one accounts for alternating on-site energies, the third term is the Zeeman coupling (magnetic field $B = g\mu_B H$) and the last term is the Rashba SO coupling (strength α_R). We consider a finite chain of length L which is connected to left and right leads by tunneling amplitudes T_l and T_r , respectively. Note that we investigate here the case of *nonmagnetic leads*. We assume that the SO coupling vanishes in the leads and that the magnetic field only affects the central region significantly.

III. THE SPECTRUM

To understand the magneto transport results it is useful to first consider the spectrum of (1). For clarity all spectra are plotted in the reduced Brillouin zone $k \in [-\pi/2a, \pi/2a]$ associated with the presence (possibly small) of alternating on site energies. Typically this

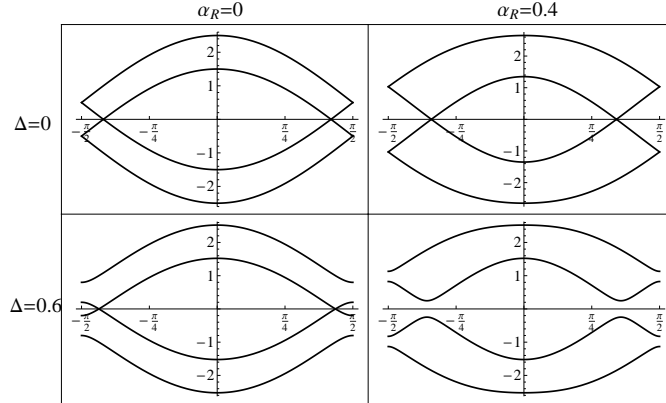


FIG. 2: Spectrum of the tight-binding chain (see Eqs. (1)-(2)) with magnetic field ($B = g\mu_B H = 1.3$), with and without Rashba coupling α_R and ionicity Δ ($t = 1$ has been taken as unit of energy).

spectrum consists of 4 branches and it can be obtained exactly:

$$E_{1/2}^{\pm}(k) = \pm \sqrt{4\alpha_R^2 \sin^2 k + \frac{B^2}{4} + \frac{\Delta^2}{4} + 4t^2 \cos^2 k \pm W}$$

$$W = \sqrt{16\alpha_R^2 t^2 \sin^2(2k) + 4B^2 t^2 \cos^2 k + \frac{B^2 \Delta^2}{4}} \quad (2)$$

in the general case with spin-orbit coupling α_R and in the presence of a magnetic field. It is shown in Fig. 2 for different cases of Δ and α_R , with a non-zero magnetic field B .

The upper left corner of Fig. 2 depicts the trivial case of a non dimerized tight binding chain ($\Delta = 0$) in the presence of a magnetic field. The latter gives rise to a splitting between the spin up and spin down bands. The spectrum has been folded in this reduced Brillouin zone to serve as a point of comparison for the other cases, with dimerisation.

We now consider the case of a non-zero value for Δ (bottom left plot of Fig. 2). For $\alpha_R = 0$, the spin up and down bands are still separated, but the dimerisation opens a gap for each spin band at the boundaries of the Brillouin zone. This implies that for energies close to the Fermi level only one spin channel will be open for the transport (complete spin filtering effect, see next Section). As shown on the Figure, the magnetic field can be so strong that the gap closes and the system can become metallic. We now switch on the Rashba coupling in the presence of dimerisation (bottom right corner of Fig. 2). In this case, the coupling between spin up and spin down gives rise to an anticrossing, so that the spin-orbit coupling opens up a gap again.

On the other hand, there is no spin filtering effect for a homogeneous, metallic chain

($\Delta = 0$, top row of Fig. 2). Without magnetic field (not shown), the spin-orbit coupling can be taken exactly into account by a shift of $k \rightarrow k + \arctan(\alpha_R/t)$. As can be easily inferred from the spin split band structure in a magnetic field (left plot) the density of states for spin up and spin down electrons is the same in that case. And the introduction of spin-orbit coupling (right plot) does not open a gap. This proves that both effects, i.e. the complete spin filtering effect and the spin-orbit driven metal-insulator transition cannot be observed in a metallic system ($\Delta = 0$).

IV. TRANSPORT THROUGH A FINITE CHAIN

In the absence of electronic interactions, the current through a finite chain of length L can be cast exactly in a Landauer type formula, written here for zero temperature. This current depends on the orientation of electrons spin at the input lead and the output lead: the current $I_{ss'}$ for instance, corresponds to electrons which enter with spin s (with $s = \uparrow$ or \downarrow) from the left lead and leave the current channel with spin s' to the right lead. With this convention,

$$I_{ss'}(V_D) = \Gamma_L \Gamma_R \int_{\mu_L}^{\mu_R} dE \left| G_{ab}^{ss'}(E) \right|^2. \quad (3)$$

The integration is performed between the chemical potentials of the left and right leads ($\mu_L = -V_D$ and $\mu_R = 0$). The energy dependent transmission is simply proportional to the square modulus of the total retarded Green function of the chain (which include the coupling with the leads) between both endpoints, noted here a and b . The tunneling rates on the left and right side are defined as $\Gamma_j \equiv 2\pi\rho_j T_j^2$ ($j = L, R$), where ρ_j is the (constant) density of states of lead j , and T_j the tunneling amplitude to lead j . The total Green function of the chain between the end sites a and b , $G_{ab}^{ss'}$ can be obtained from the Green function of the bare chain (uncoupled to leads) $g_{ab}^{ss'}$ by solving the Dyson equations:

$$\begin{pmatrix} G_{ab}^{\uparrow\uparrow} \\ G_{ab}^{\downarrow\uparrow} \\ G_{bb}^{\uparrow\uparrow} \\ G_{bb}^{\downarrow\uparrow} \end{pmatrix} = \begin{pmatrix} g_{ab}^{\uparrow\uparrow} \\ g_{ab}^{\downarrow\uparrow} \\ g_{bb}^{\uparrow\uparrow} \\ g_{bb}^{\downarrow\uparrow} \end{pmatrix} + \begin{pmatrix} g_{aa}^{\uparrow\uparrow} & g_{aa}^{\uparrow\downarrow} & g_{ab}^{\uparrow\uparrow} & g_{ab}^{\uparrow\downarrow} \\ g_{aa}^{\downarrow\uparrow} & g_{aa}^{\downarrow\downarrow} & g_{ab}^{\downarrow\uparrow} & g_{ab}^{\downarrow\downarrow} \\ g_{ba}^{\uparrow\uparrow} & g_{ba}^{\uparrow\downarrow} & g_{bb}^{\uparrow\uparrow} & g_{bb}^{\uparrow\downarrow} \\ g_{ba}^{\downarrow\uparrow} & g_{ba}^{\downarrow\downarrow} & g_{bb}^{\downarrow\uparrow} & g_{bb}^{\downarrow\downarrow} \end{pmatrix} \begin{pmatrix} \Sigma_a G_{ab}^{\uparrow\uparrow} \\ \Sigma_a G_{ab}^{\downarrow\uparrow} \\ \Sigma_b G_{bb}^{\uparrow\uparrow} \\ \Sigma_b G_{bb}^{\downarrow\uparrow} \end{pmatrix}$$

and similar equations for the opposite spins, and where $\Sigma_j = -i\Gamma_j$ is the retarded self-energy coming from the coupling to lead $j = L, R$. The Green functions of the bare chain $g_{ab}^{ss'}$ are

obtained simply by computing the eigenvalues and eigenstates of the finite chain, and using a spectral representation:

$$g_{ab}^{ss'}(E) = \sum_n \frac{\psi_n^s(a) (\psi_n^{s'}(b))^*}{E - E_n + i0^+} \quad (4)$$

Here all the Green functions, and consequently the current in Eq. (3), are 2x2 matrices in spin space. This is a consequence of the Rashba SO coupling, which couples the spin-up and spin-down channels. Without SO coupling all quantities become diagonal in spin space, and the formula for the total Green function reduces to:

$$G_{ab}^{ss} = \frac{g_{ab}^{ss}}{(1 - \Sigma_L g_{aa}^{ss})(1 - \Sigma_R g_{bb}^{ss}) - \Sigma_L \Sigma_R g_{ab}^{ss} g_{ba}^{ss}} \quad (5)$$

Let us start the discussion of our numerical results with the current-voltage characteristics in a magnetic field with $\Delta \neq 0$, but without SO coupling (see Fig. 3). The magnetic field $B = B_c$ is chosen such that it just closes the gap, but the exact value of this parameter is nevertheless not important for the *spin-filtering effect*. The transport for drain voltages between $V_D = 0$ and $V_D \simeq 0.6t$ is only possible for one spin channel. It means that we find complete spin polarization in the transport channel (connected to nonmagnetic leads) and a complete spin-filtering. The spin polarization of the current is defined in the general case as^{7,14}

$$P = \frac{I_{\uparrow\uparrow} + I_{\downarrow\uparrow} - I_{\uparrow\downarrow} - I_{\downarrow\downarrow}}{I_{\uparrow\uparrow} + I_{\downarrow\uparrow} + I_{\uparrow\downarrow} + I_{\downarrow\downarrow}}. \quad (6)$$

As shown on Fig. 3, the spin polarization remains finite (but smaller than unity) for larger voltages (between approximatively $0.6 t$ and $2.25 t$) and disappears at approximatively $2.25 t$ where the current reaches saturation (all the electrons of the tight-binding band contribute). A finite spin polarization means also that the current creates a total magnetization M in the transport channel of length L . The value of the total magnetization is given by $M/\mu_B = L(I_{\uparrow\uparrow} + I_{\downarrow\uparrow} - I_{\uparrow\downarrow} - I_{\downarrow\downarrow})/\langle v \rangle$, where $\langle v \rangle$ means the average velocity of the electrons which are active in the transport process (ballistic transport).

This spin-filtering effect is expected to work for a wide range of gap values. The voltage region where only one spin channel is open is determined by the applied magnetic field. This works also if the magnetic field is not sufficiently strong to close the gap. Therefore, even materials with gap values of about 0.5 eV are possible candidates to show the complete spin-filtering effect. The onset of the minority spin channel (at zero energy in Fig. 3) is given by the relative position of the chemical potential with respect to the upper band edge

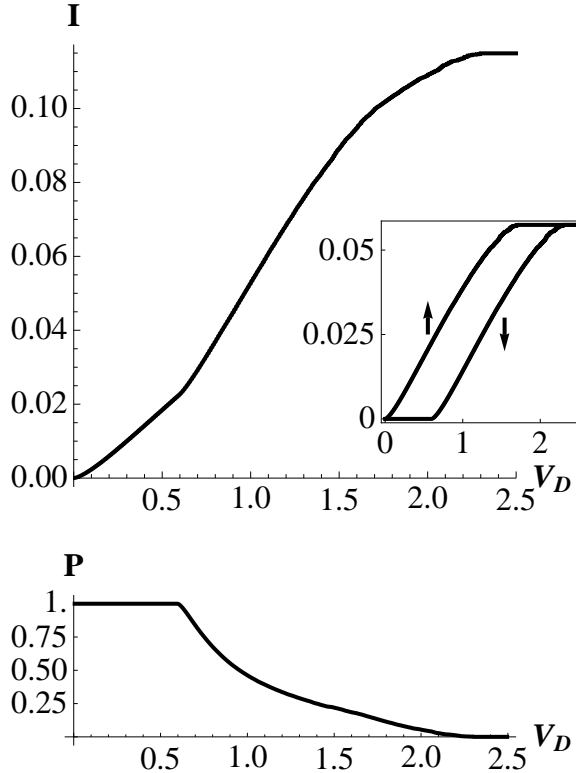


FIG. 3: Upper plot: total current as a function of the bias voltage V_D , in the *spin filtering* configuration. $\Delta = 0.6$, $B = 0.6$, $\Gamma_L = \Gamma_R = 0.1$ and $t = 1$, for a chain of 500 sites. The inset shows the separate contributions from the spin-up and spin-down current. Lower plot: spin polarization (Eq. (6)) for the same parameters.

of the valence band which may vary from one experimental situation to another.

We now consider the case of non-zero SO coupling. The transition from metallic to insulating behavior driven by SO coupling is shown in Fig. 4. The magnetic field is the same as in Fig. 3, i.e. it just closes the gap $B = B_c = \Delta$, and the Rashba SO coupling is $\alpha_R = 0.2t$. It is created by an external gate voltage (see Fig. 1). The SO coupling leads to an insulating behavior, as seen in the spectrum (Fig. 2) and in the current-voltage characteristics (Fig. 4). In contrast to Fig. 3, the presence of the SO coupling α_R leads to a current on-set at $V_D \simeq 0.25t$ corresponding to half of the gap value for our choice of the chemical potential. The different current components $I_{ss'}$ are now all different, and the spin polarization (Eq. 6) is different from zero but not complete ($0 < P < 1$).

Note that the relative values of the different spin-components of the current in Fig. 4 are

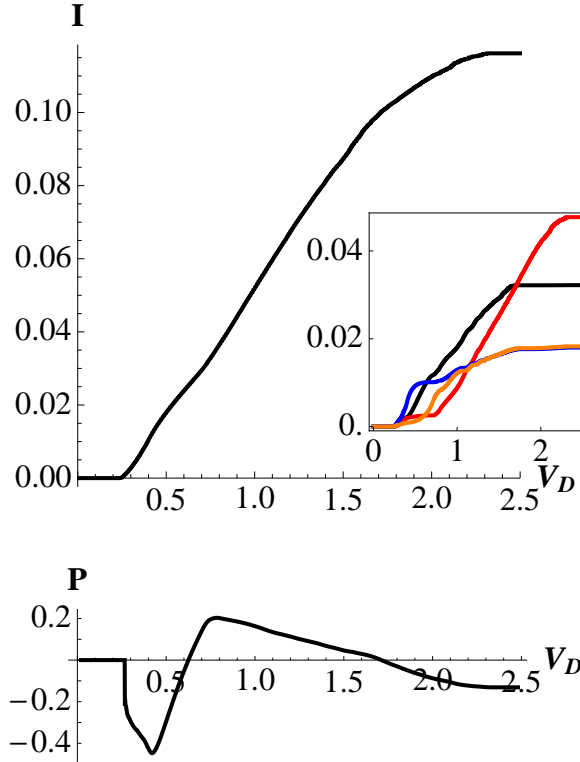


FIG. 4: (Color online) Upper plot: total current as a function of the bias voltage V_D , in the presence of Rashba spin-orbit coupling, with $\alpha_R = 0.2$, $\Delta = 0.6$, $B = 0.6$, $\Gamma_L = \Gamma_R = 0.1$ and $t = 1$ for a chain of 500 sites. The inset shows the four spin components of the current (in this order from top to bottom near $V_D = 2.5$): $I_{\downarrow\downarrow}$ (red), $I_{\uparrow\uparrow}$ (black), $I_{\downarrow\uparrow}$ (orange), and $I_{\uparrow\downarrow}$ (blue). Lower plot: spin polarization (Eq. (6)) for the same parameters.

dependent on the chain length. This is due to the Rashba SO coupling, which is known to induce spin precession. Here, this spin precession is made more complex due to the presence of the magnetic field B and the ionicity Δ . The oscillations of the current components, as a function of the chain length L , are shown in Fig. 5, for L varying between 500 and 600. These oscillations have a rather small contrast, show several periods and a complicated dependence on bias voltage V_D in the general case (a dominating period seems to be present for the off diagonal components of the current though). This has to be contrasted with the pure metallic case ($B = 0$ and $\Delta = 0$, shown in the inset of Fig. 5), where only one period $L_p = \pi/\alpha$ is present independently on V_D , and where the contrast is maximum.

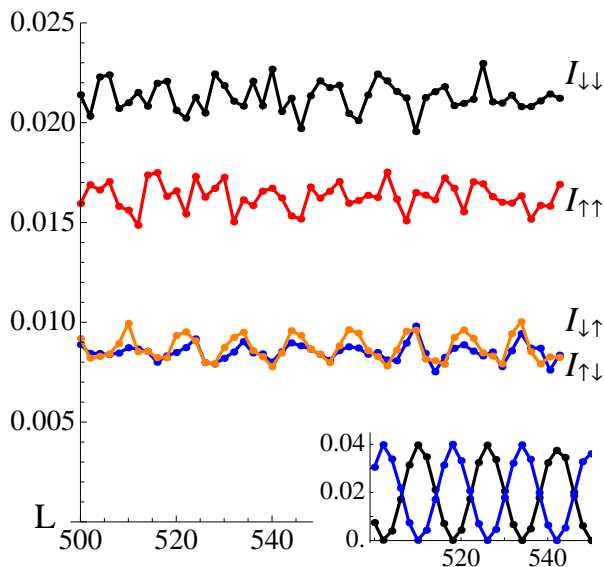


FIG. 5: (Color online) Oscillations of the spin components of the current as a function of the chain length (lengths between 500 and 600), for $V_D = 2.0$, when SO Rashba coupling is present ($\alpha_R = 0.2$, $\Delta = 0.6$, $B = 0.6$, $\Gamma_L = \Gamma_R = 0.05$ and $t = 1$). Inset: the same plot with $B = 0$ and $\Delta = 0$, where $I_{\uparrow\uparrow} = I_{\downarrow\downarrow}$ and $I_{\uparrow\downarrow} = I_{\downarrow\uparrow}$

V. CONCLUSIONS

In studying the combined effect of magnetic field and SO interaction on the transport in 1D band insulators we found two interesting effects. First, already without SO coupling, the presence of a magnetic field leads to complete spin filtering. We studied this effect here by connecting the conduction channels to nonmagnetic leads but the effect of magnetic leads is easy to imagine, at least qualitatively. Then, spin filtering means high conductance for parallel magnetization in the leads and low conductance for antiparallel arrangement.

We speculate that the voltage region of the spin filtering effect may be dramatically enhanced by the presence of magnetic impurities in the band insulator, due to the giant Zeemann effect. This might be important for the experimental verification of our proposal.

The second striking effect of this study appears in band insulators with small band gap that may be closed by a magnetic field. In that situation, the SO coupling leads again to an insulating behavior. That is especially interesting for the Rashba spin orbit coupling which is tuned by a gate voltage. Therefore, we may propose a device in which the metal-

insulator transition is controlled by the gate voltage via the Rashba SO term. This is in sharp contrast with 1D metallic systems, where the SO coupling does not lead to any metal-insulator transition.

We also showed the oscillations of the different current components with the chain length. Whereas the simple oscillations in metallic systems are easy to understand, the oscillations are much more complex for band insulators. We have left a detailed analysis of these oscillations for further studies. In our calculations the band insulator was simulated by an ionic term of alternating on-site energies in the Hamiltonian. But we think that our results are generic to any kind of band insulator. On the other hand, the way in which Coulomb correlations influence our results may be different from one microscopic Hamiltonian to another. We expect that the Coulomb correlation just scales the band gap (either to larger or to smaller values) and that the presented results should remain valid with effective parameters, however.

The authors thank Marc Bescond and Alvaro Ferraz for useful discussion.

-
- ¹ A. Fert, Rev. Mod. Phys. **80**, 1517 (2009).
² S. Datta and B. Das, Appl. Phys. Lett. **56**, 665 (1990).
³ G. Dresselhaus, Phys. Rev. **100**, 580 (1955).
⁴ E.I. Rashba, Fiz. Tverd. Tela (Leningrad) **2**, 1224 (1960) [Sov. Phys. Solid State **2**, 1109 (1960)].
⁵ A.V. Moroz, K.V. Samokhin, and C.H.W. Barnes, Phys. Rev. B **62**, 16900 (2000); *ibid* Phys. Rev. B **62**, 16900 (2000).
⁶ W. Häusler, Phys. Rev. B **63**, 121310(R) (2001).
⁷ P. Středa and P. Šeba, Phys. Rev. Lett. **90**, 256601 (2003).
⁸ A. Iucci, Phys. Rev. B **68**, 075107 (2003).
⁹ V. Gritsev, G.I. Japaridze, M. Pletyukhov, and D. Baeriswyl, Phys. Rev. Lett. **94**, 137207 (2005).
¹⁰ P. Foldi, B. Molnar, M.G. Benedict, and F.M. Peeters, Phys. Rev. B **71**, 033309 (2005).
¹¹ F. Cheng and G. Zhou, Journal of Physics: Condensed Matter **19**, 136215 (2007).
¹² M. Scheid, M. Kohda, Y. Kunihashi, K. Richter, and J. Nitta, Phys. Rev. Lett. **101**, 266401 (2008).

- ¹³ S. Bellucci and P. Onorato Phys. Rev. B **78**, 235312 (2008).
- ¹⁴ J.E. Birkholz and V. Meden, Jour. Phys.: Condensed Matter **20**, 085226 (2008); *ibid*, Phys. Rev. B **79**, 085420 (2009).
- ¹⁵ G.I. Japaridze, H. Johannesson and A. Ferraz, unpublished, arXiv:0904.1846 (2009).
- ¹⁶ Z. Ristivoyevic, G.I.Japaridze and T. Nattermann, unpublished (2009).
- ¹⁷ M.J. Rice and E.J. Mele, Phys. Rev. Lett. **49**, 1455 (1982).
- ¹⁸ W.P. Su, J.R. Schrieffer, and A.J. Heeger, Phys. Rev. Lett. **42**, 1698 (1979).
- ¹⁹ N. Hamada, S.I. Sawada, and A. Oshiyama, Phys. Rev. Lett. **68**, 1579 (1992).
- ²⁰ N.B. Brandt and E.A. Svistunova, Sov. Phys. Uspekhi **101** 249 (1970).